Wall Pressure Fluctuations in Attached Boundary-Layer Flow

A. L. Laganelli* and A. Martellucci†
Science Applications, Inc., Wayne, Pennsylvania
and
L. L. Shaw‡
AFWAL/FIBE, Wright-Patterson Air Force Base, Ohio

An examination has been made to derive a correlation for an aeroacoustic environment associated with attached compressible flow conditions. It was determined that fluctuating pressure characteristics described by incompressible theory as well as empirical correlations could be modified to a compressible state through a transformation function. In this manner, compressible data were transformed to the incompressible plane where direct use of more tractable prediction techniques are available for engineering design analyses. The investigation centered on algorithms associated with pressure magnitude and power spectral density. The method and subsequent prediction techniques are shown to be in excellent agreement with both incompressible and compressible flow data.

Nomenclature

A = parameter, $1.7 < A < 3$, incompressible flow
C_f = skin friction coefficient
l = characteristic length
m = viscous power law exponent
M = Mach number
MF = Mangler factor
n = velocity power law exponent
P_{rms} = measured root mean square (rms) acoustic pressure
Pe = local boundary-layer static pressure
q = dynamic pressure
r = recovery factor (0.896 for turbulent flow)
Re = Reynolds number
T = temperature
u = velocity in stream directions
V = characteristic velocity
δ^* = boundary-layer displacement thickness
ϵ_T = compressibility factor
μ = dynamic viscosity
ρ = density of fluid
σ = theoretical value of rms fluctuating pressure ($0-\infty$ Hz)
τ = shear stress
Υ = ratio of specific heats (1.4 for air)
ψ = power spectral density
ω = frequency, rad/s

Subscripts

aw = adiabatic wall
c = compressible
e = evaluated at edge of boundary layer
i = incompressible
s = based on wetted length
w = wall
∞ = freestream conditions

Superscript

$( )^*$ = based on reference temperature conditions

Presented as Paper 81-1227 at the AIAA 14th Fluid and Plasma Dynamics Conference, Palo Alto, Calif., June 23-25, 1981; submitted July 14, 1981; revision received March 17, 1982.

*Manager, Applied Systems Technology Division. Member AIAA.
†Operations Manager, Applied Mechanics Operations. Member AIAA.
‡Aerospace Engineer, Acoustics and Sonic Fatigue Group. Member AIAA.

Introduction

HIGH-performance ballistic vehicles are subject, during re-entry, to an intense fluctuating pressure field which can affect the integrity of the vehicle structure and impose adverse vibration levels on internal components. These pressure fluctuations arise from instability and unsteady motions of fluid which focus on intermittent eruptions of the viscous sublayer. Pressure fluctuations in an incompressible flow have classically been examined by relating the phenomenon to velocity fluctuations through Poisson's equation. Moreover, further simplification has been invoked by considering only an interaction of the turbulent structure and mean shear stresses. In this manner, mean square pressure fluctuations for attached flows have been predicted. However, the phenomenon is still understood only vaguely, and design criteria have been developed primarily on the basis of experimental data.

An examination of the literature has revealed that considerable work has been devoted to incompressible flowfields as well as compressible flow in the supersonic and, more recently, hypersonic flow range. The present study will be concerned with supersonic/hypersonic attached turbulent boundary-layer flow characteristics. Moreover, this investigation considers the development of a correlation to predict pressure magnitude and power spectral density (PSD) based on experimental data and theory. The latter is derived from incompressible flow characteristics and subsequently modified to compressible flow behavior using transformation functions. These techniques have been successfully used in boundary-layer prediction methods and verified by experimental evidence.

The objective of the present investigation is to provide a definition of the fluctuating pressure environment, in terms of design algorithms, for the purpose of predicting vehicle structural and internal component response. This paper has been abstracted, in part, from a very comprehensive study performed by Laganelli and Howe[1] who conducted an analytical and experimental program to define aeroacoustics environment applicable to re-entry vibration response analysis.

Previous Work

As previously noted, this study will emphasize supersonic/hypersonic attached turbulent flow behavior. Readers interested in subsonic flow conditions are referred to the survey of Willmarth[2] as well as Refs. 1 and 3. Moreover, the correlations describing the aeroacoustic environment associated with pressure magnitude and power spectral density will be addressed. As such, the works of Refs. 1 and 4 will be the starting point of this investigation.

Lilley[5] found that the normalized power magnitude for subsonic conditions was bound in the range $1.7<\sigma/\tau_w<3$ at $M_\infty<1$; whereas, for a compressible flow, the ratio σ/τ_w ranged from 2.2 at zero Mach number to 5.6 at a Mach number of 10. The above limits were experimentally observed by Raman,[3] Kistler and Chen[6] and Martellucci et al.[7] as well as the recent work of Ref. 1. These investigators noted that the ratio appeared to be a weak function of the Reynolds number and Mach number. Based upon the above premise, the ratio can be expressed as

$$\sigma/\tau_w = A \tag{1}$$

where A is a parameter.

Using the definition of skin friction coefficient together with dynamic pressure, the wall shear stress can be expressed as $\tau_w = 2q_e(C_f/2)$, which when generalized to include a variable velocity power law together with the Blasius form of skin friction[8] gives

$$C_f/2 = MFK(n)\epsilon_T(Re_s)^{-2/(3+n)} \tag{2}$$

where MF is the Mangler factor (unity for flat plates), $K(n)$ is a parameter (0.0296 for 1/7 velocity power law), and the compressibility factor is defined as

$$\epsilon_T = (\rho^*/\rho_e)^{(1+n)/(3+n)}(\mu^*/\mu_e)^{2/(3+n)} \tag{3}$$

In the above, starred properties are based on the classic Eckert reference temperature method, namely,

$$T^*/T_e = \tfrac{1}{2}(1+T_w/T_e) + 0.22r[(\gamma-1)/2]M_e^2 \tag{4}$$

which in effect represents an average distribution through the boundary layer.

If one considers a constant-pressure boundary layer and the equation of state, $\rho^*/\rho_e = (T_e/T^*)$, the Sutherland viscosity law is generalized to give[9]

$$\mu^*/\mu_e = (T^*/T_e)^m \tag{5}$$

where

$$m = \frac{3}{2} + \frac{\ln[(T_e+198.6)/(T_w+198.6)]}{\ln(T_w/T_e)} \tag{6}$$

The compressibility factor can than be expressed as

$$\epsilon_T = (T^*/T_e)^{[2m-(1+n)]/(3+n)} \tag{7}$$

where T^*/T_e is given by Eq. (4). The Mangler factor, subject to the arbitrary velocity exponent, becomes[8]

$$MF = [2(2+n)/(1+n)]^{2/(3+n)} \tag{8}$$

and Eqs. (1) and (2) are written as

$$\frac{\sigma}{q_e} = 2AK(n)MF(n)\Big/\left\{Re_s^{2/(3+n)}\left[\frac{1}{2}\left(1+\frac{T_w}{T_e}\right) + 0.22r\frac{\gamma-1}{2}M_e^2\right]^{\frac{2m-(1+n)}{(3+n)}}\right\} \tag{9}$$

An examination of Eq. (9) indicates that the state of the flow development (i.e., the laminar/transitional/turbulent, where $n=7$ represents a fully developed turbulent boundary layer) will not change the rms pressure inasmuch as the ratio $K(n)MF(n)/Re_s^{2(3+n)}$ is essentially invariant for all values of n. Hence, variations in rms pressure will be a consequence of changes in the parameter A, Mach number, or wall temperature ratio. For subsonic flow conditions $M_e \to 0$ and $T_w/T_e \to$ unity and Eq. (9) can be expressed as

$$\frac{\sigma}{q_e} = \frac{2AK(n)MF(n)}{Re_s^{2/(3+n)}} \to 0.006$$

which represents the incompressible value obtained from experimental data, a result noted by several authors.[1,4,10,11]

When assessing the sensitivity of the velocity power law exponent n and the viscous power law exponent m, it was found that the state of development of the turbulent boundary layer had no effect on terms that constitute the empirical constant 0.006. The most significant effect of the power law exponents was determined to be on the compressibility parameter, in particular for hypersonic flow conditions. For example, if m is allowed to vary between 0.6 (typical flight data value) and 1.0 (0.9 is a typical wind-tunnel value) with a fixed value of n and a range of T_w/T_e, it was determined[1] that low Mach number cases showed a small variation in the compressibility factor ($\simeq 10\%$) due to changes in m, a result noted by other analysts.[9-12] However, for hypersonic conditions ($M>5$), variations in the exponent m resulted in significant departures in the compressibility factor (as high as 50%).

If, on the other hand, one fixes the value of m and Mach number (for an adiabatic wall situation), a variation in the velocity power law exponent indicated only a 6% change from $M_\infty = 4$ to 10. Consequently, with the exception of the choice of parameter A, the most significant effect in use of the compressibility parameter appears to be in the coupling of density and viscosity as opposed to density changes alone, a

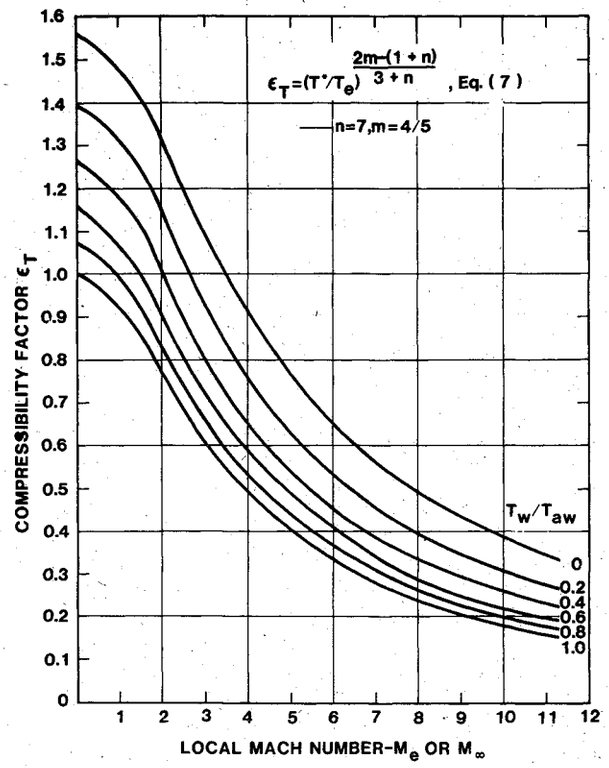

Fig. 1 Variation of compressibility factor with Mach number and wall temperature.

result that appears to be amplified for high Mach number values.

Equation (9) can now be expressed as

$$(\sigma/q_e)_c = (\sigma/q_e)_i \epsilon_T \tag{10}$$

where the subscripts c and i imply compressible and incompressible conditions, respectively. The compressibility parameter ϵ_T is defined by Eq. (7). Moreover, the use of the compressible parameter allows one to transform compressible data into the incompressible plane where direct use of more tractable prediction techniques are available for engineering design analysis. This approach has been successfully demonstrated in fluid dynamic phenomenology.

Equation (10) can be expressed in limiting cases which are more recognizable in the literature. For example, if one considers a recovery factor $r=0.9$ and $\gamma=1.4$ (air) together with the definition of the recovery temperature

$$T_{aw}/T_e = 1 + r[(\gamma-1)/2]M_e^2$$

Equation (10) can be written as

$$\sigma/q_e = 0.006/[\tfrac{1}{2} + (T_w/T_{aw})(\tfrac{1}{2} + 0.09M_e^2) + 0.04M_e^2]^{0.64} \tag{11}$$

where $(\sigma/q_e)_i$ is 0.006 and the power law exponents where chosen are $n=7$ and $m=4/5$, respectively. The limiting cases for Eq. (11) are the adiabatic wall case ($T_w = T_{aw}$, hot-wall condition) and the cold-wall case ($T_w \ll T_{aw}$).

Discussion of Results

Figure 1 shows the compressibility factor as a function of Mach number with wall temperature as a parameter. It is quite interesting to note that the incompressible data ($M<1$) could reflect wall temperature variations for $T_w/T_{aw}<1.0$. The curves were generated using a fully developed turbulent boundary power law profile ($n=7$) and an average viscous power law exponent (4/5) which is typical of wind tunnel data.

Figure 2 shows Eq. (11) compared to the predictions of Lowson[10] (adiabatic) and Houbolt[11] (cold wall). It should be noted that Houbolt modified his cold-wall prediction to an adiabatic result, which is essentially the same as Lowson. However, in neither case of Refs. 10 and 11 were viscous effects considered. Also shown are data from several experimental studies for both incompressible and compressible flows. While a large scatter is evident in the data, the effects of viscosity and wall temperature appear significant with increasing Mach number. This is believed to be a consequence of the increasing rms pressure resulting from the viscous layer adjacent to the wall.

Equation (11) can be cast into a different format which shows the magnitude of the rms pressure relative to the local static value. Here, one uses the definition of the dynamic pressure $q_e = \gamma/2 P_e M_e^2$ such that

$$(\sigma/p_e)_c = \frac{0.006\gamma/2M_e^2}{[\tfrac{1}{2} + (T_w/T_{aw})(\tfrac{1}{2} + 0.09M_e^2 + 0.04M_e^2)]^{0.64}} \tag{12}$$

Figure 3 shows the normalized rms pressure as a function of Mach number for the two limiting cold-wall ($T_w \ll T_{aw}$) and hot-wall ($T_w = T_{aw}$) conditions. Data from several experiments are shown as well as freestream noise measurements and surface data obtained in a laminar boundary layer (LBL). Good agreement is noted for the fully developed turbulent flow conditions. Moreover, the theory predicts the correct trend. It is interesting to note the difference in level of the rms pressure between freestream measurements to cone surface measurements in a laminar boundary layer in the work of Stainback et al.[13] The authors noted that at low shock strengths, the model shock had little effect on the ratio of rms sound pressure and local pressure and that the disturbances behind the shock are still predominantly sound. Also, fluctuating pressure levels measured underneath the laminar portion of the boundary layer differed significantly for the various facilities where data were obtained. An examination of the unpublished measurements of Donaldson[14] and Laderman[15] indicates a high level of tunnel noise when compared to the cone data of

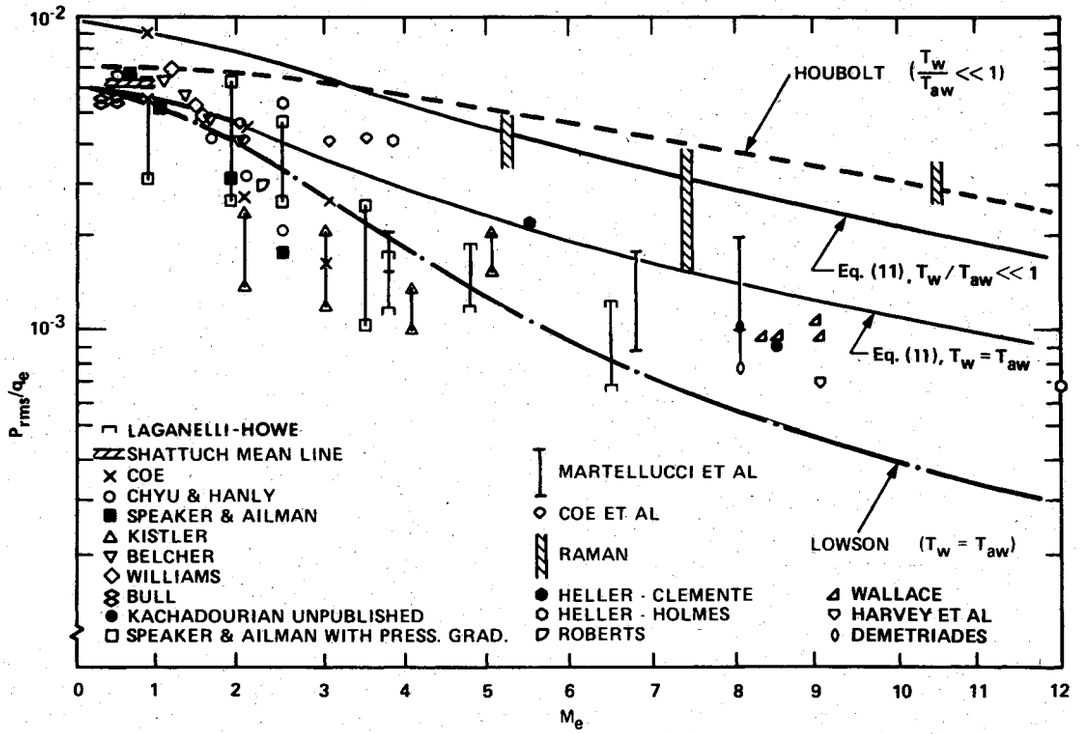

Fig. 2 Comparison of theory with data for rms pressure-attached turbulent boundary-layer flow.

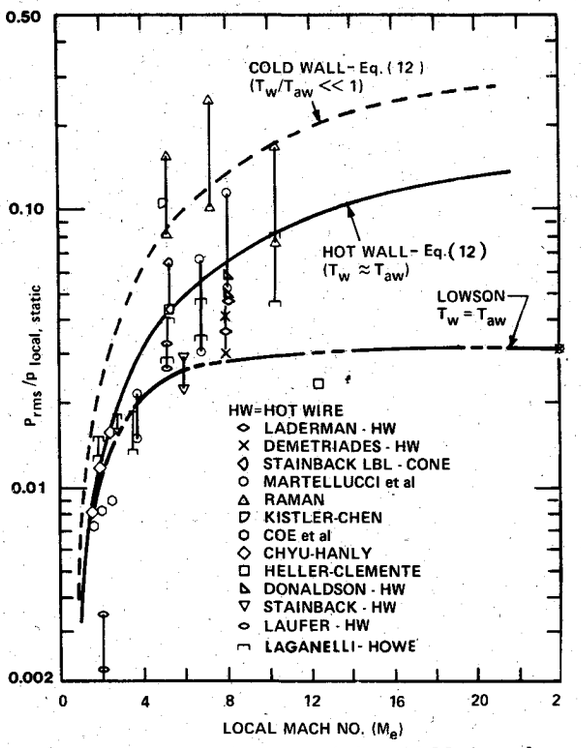

Fig. 3 Normalized rms pressure variation with Mach number.

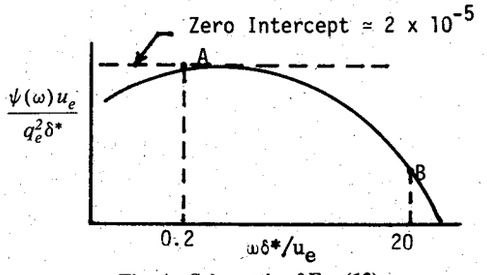

Fig. 4 Schematic of Eq. (13).

Ref. 7 ($M_e \simeq 6.7$) which were obtained in the same facility. Inasmuch as the measured levels of normalized rms pressure in laminar flow were shown to be higher than turbulent/transitional levels, one must speculate on possible shock attenuation effects.

A final word on the rms pressure prediction schemes as related to measured data is in order, in particular, the power law exponents. It is generally accepted that the velocity power law exponent n of 7 is accepted for fully developed turbulent flow. However, Laganelli et al.[8] have shown that fully developed turbulent conditions could not be attained even on models 1.5 m (5 ft) long. More realistically, the value of n, as determined from profile measurements, was approximately 9 and this parameter reached values as high as 16 just after transition. If a value of $n=9$ and $m=0.8$ were used, the ratio σ/q_e would reduce by approximately 15%. If higher values were chosen, the ratio σ/q_e could be reduced by 25% and approach the Lawson prediction shown in Fig. 2.

Power Spectral Density Considerations

Houbolt[11] examined the compressible data of several early experiments and noted that the spectra could be represented by the empirical formula

$$\frac{\psi(\omega)u_e}{q_e^2\delta^*} = \frac{2\times 10^{-5}}{1+(\omega\delta^*/u_e)^2} \tag{13}$$

in the range of $0.2<\omega\delta^*/u_e<20$ which is schematically represented in Fig. 4. Inasmuch as the data indicate a peak in the low-frequency range (point A), the empirical representation was considered to be flat in this range. This situation is considered a conservative approach in structural applications where low-frequency responses ($f<1000$ Hz) tend to predominate. From the definition of the mean square pressure and utilizing Eq. (13), there results

$$\sigma^2 = p_{\text{rms}}^2 = \int_0^\infty \psi(\omega)\,d\omega = 2\times 10^{-5}\frac{\pi}{2}q_e^2$$

Here, we note that the constant $\pi/2$ is a consequence of the functional form of the empirical formula representing the spectrum. Normalized rms pressure is determined to be $\sigma/q_e = 0.0056$ which is approximately the value of measured incompressible flow data.

On the basis of the above development, it appears that a reasonable approach to evaluate empirical formulas for power spectral density is to assess the zero frequency intercept value and the normalized rms pressure values resulting from integration of the various equations. Moreover, the incompressible data of Bull[16] and Blake[17] will be used as a baseline for testing the techniques. It should be noted that these data have been well documented and reviewed in the scientific community. Moreover, the recent assessment of these data by Willmarth[2] and counterargued by Bull and Thomas[18] indicate the credibility of the Bull[16] data for a baseline case.

To integrate the various empirical power spectral density equations, consider the following definite integral

$$\int_0^\infty \frac{x^{r-1}}{(p+qx^s)^{n+1}}\,dx = \frac{1}{sp^{n+1}}\left(\frac{p}{q}\right)^{r/s}\frac{\Gamma(r/s)\Gamma[1+n-(r/s)]}{r(1+n)} \tag{14}$$

for the condition $0<r/s<n+1$. In the above $\Gamma(z)$ is the gamma function $=\int_o^\infty e^{-t}t^{z-1}dt$. The three equations to be evaluated are from the works of Houbolt,[11] Lowson,[10] and Robertson[19] and will be designated as H, L, and R, respectively. Considering incompressible flow and the format of Eq. (13), the three equations become

$$\left.\frac{\psi(\omega)u_\infty}{q_\infty^2\delta^*}\right|_H = \frac{\bar{\psi}(0)}{1+(\omega\delta^*/u_\infty)^2}$$

$$\left.\frac{\psi(\omega)u_\infty}{q_\infty^2\delta^*}\right|_L = \frac{\bar{\psi}(0)}{[1+(\omega\delta^*/u_\infty)^2]^{3/2}}$$

$$\left.\frac{\psi(\omega)u_\infty}{q_\infty^2\delta^*}\right|_R = \frac{2\bar{\psi}(0)}{[1+(2\omega\delta^*/u_\infty)^{0.9}]^2}$$

where $\bar{\psi}(0)$ is the normalized zero intercept (low-frequency) value of the power spectra. Figure 5 shows the data of Bull,[16] Blake,[17] and Schloemer.[20] It appears that the intercept value of the Bull data is approximately 2.2×10^{-5}, while that of Blake approximately 1.3×10^{-5}.

If we consider the definition of the rms pressure and integrate each of the above expressions, there results

$$\left(\frac{\sigma}{q_\infty}\right)_H^2 = \frac{\pi}{2}\bar{\psi}(0);\quad \left(\frac{\sigma}{q_\infty}\right)_L^2 = \bar{\psi}(0);\quad \left(\frac{\sigma}{q_\infty}\right)_R^2 = \sqrt{\pi}\bar{\psi}(0)$$

which yield, respectively

$$\left(\frac{\sigma}{q_\infty}\right)_H = 0.0056;\quad \left(\frac{\sigma}{q_\infty}\right)_L = 0.00447;\quad \left(\frac{\sigma}{q_\infty}\right)_R = 0.00471$$

Hence, it appears that the Houbolt functional form best represents the measured incompressible normalized rms pressure data. Relative to the zero intercept value, if we allow σ/q to take on the value of 0.006 and consider the following

$$\frac{\psi(\omega\to 0)u}{q^2\delta^*} = \frac{\psi(\omega\to 0)u}{\sigma^2\delta^*}\left(\frac{\sigma}{q}\right)^2$$

then

$$\left.\frac{\psi(0)u}{q^2\sigma^*}\right|_H = \frac{2}{\pi}(3.6\times 10^{-5}) = 2.29\times 10^{-5} \rightarrow \text{Bull's data}$$

$$\left.\frac{\psi(0)u}{q^2\sigma^*}\right|_L = 3.6\times 10^{-5} > \text{Bull's data}$$

$$\left.\frac{\psi(0)u}{q^2\sigma^*}\right|_R = \sqrt{\pi}(3.6\times 10^{-5}) = 6.48\times 10^{-5} \gg \text{Bull's data}$$

Thus, considering a limiting representation ($M\to 0$) of each empirical format, it appears again that the Houbolt concept best represents the data of Bull. One should note that $\sigma/q = f[M, Re, T_w]$ and approaches a value of approximately 0.006 for incompressible flow conditions. If the Houbolt algorithm is reconsidered over the entire spectrum

$$\psi(\omega) = \frac{\psi(0)}{1+K^2\omega^2} \tag{15}$$

where $K = kl/V$, for l and V some arbitrary length and velocity and k a constant. Again using the definition of the power magnitude and Eq. (15), there results

$$\sigma^2 = \int_0^\infty \psi(\omega)\,d\omega = \frac{\psi(0)}{K}\,\frac{\pi}{2}$$

and Eq. (15) becomes

$$\frac{\psi(\omega)V}{q^2 l} = \frac{(\sigma/q)^2(2/\pi)\bar{k}}{1+(\bar{k})^2(\omega l/V)^2} \tag{16}$$

where $\bar{k} = k/2\pi$. For zero intercept values, the above is written as

$$\frac{\psi(0)v}{q^2 l} = \left(\frac{\sigma}{q}\right)^2\frac{2}{\pi}\bar{k} \tag{17}$$

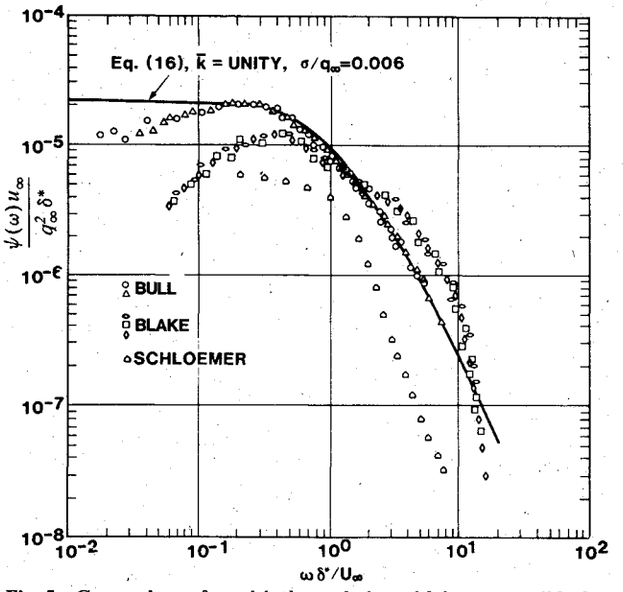

Fig. 5 Comparison of empirical correlation with incompressible data for normalized power spectral density.

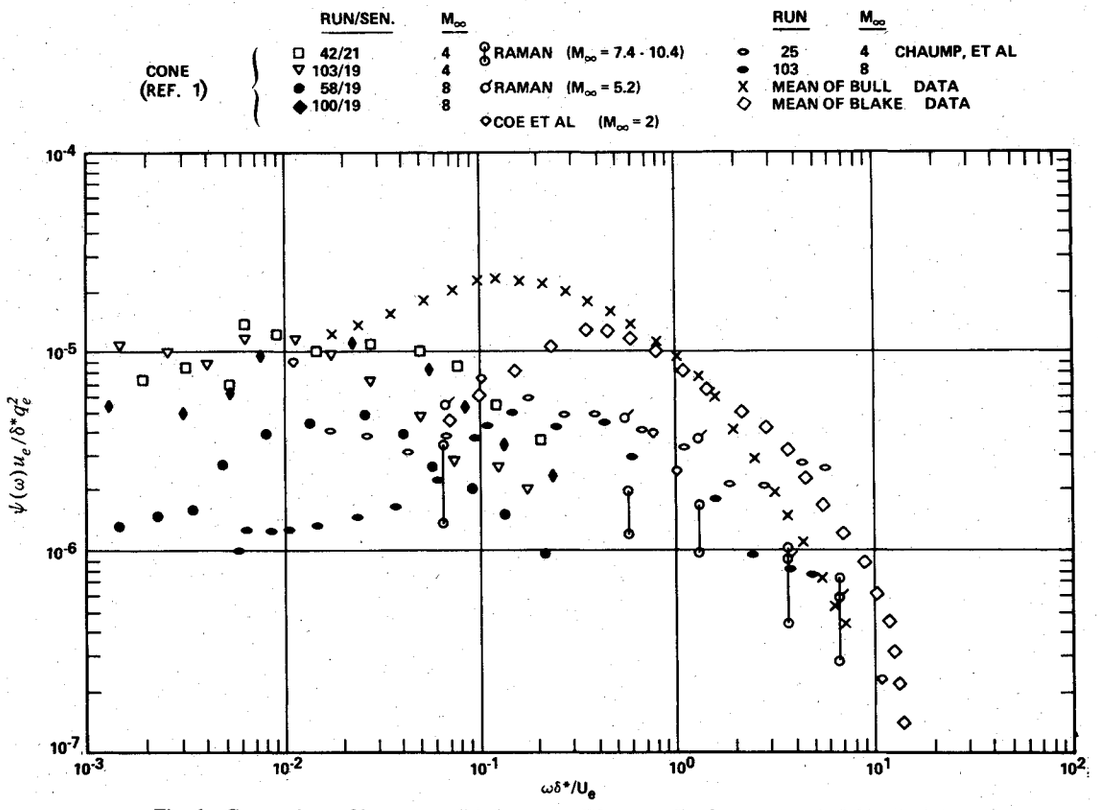

Fig. 6 Comparison of incompressible/compressible normalized power spectral density data.

Now Bull reported values of $\sigma/q=0.005$ while Blake reported values of $\sigma/q=0.00876$; the latter result is considered quite high. If we allow for $\bar{k}=$ unity, the normalized zero intercept values of PSD become 1.59×10^{-5} for Bull and 4.80×10^{-5} for Blake. One sees from Fig. 5 that these values are not in concert with the data.

In order to match the data as $\omega\to0$, $\bar{k}$ would have values of 1.3825 and 0.266 for Bull and Blake, respectively. If these values were used in Eq. (16) with the measured values of σ/q_∞, the equation would underpredict the Bull data while significantly overpredicting the Blake data. If we allowed $\sigma/q_\infty=0.006$ and $\bar{k}=$ unity (Houbolt result), the zero intercept value by Eq. (17), would be 2.29×10^{-5}, a result that matches the Bull data quite nicely. Consequently, Eq. (16) with $\bar{k}=$ unity is considered the most appropriate algorithm for predicting incompressible power spectral density.

Keeping in mind that Houbolt's functional form does not preclude compressible conditions, the following is offered as an appropriate generalization. Using Bull's data as a baseline as well as the Houbolt functional form, Eq. (16) can be written as

$$\left(\frac{\psi(\omega)u_e}{q_e^2\sigma^*}\right)_i=\frac{(\sigma/q_e)_i^2(2/\pi)\bar{k}}{1+(\bar{k})^2(\omega\delta^*/u_e)^2},\quad \bar{k}\neq\text{unity}$$

Raman[3] determined a similar expression for compressible flow that considered the functional form of Lowson. It was previously stated that the incorporation of the $(\sigma/q_e)^2$ in the above acts like a transformation function for compressible effects as given by Eq. (10). Thus, for $\omega\to0$, we can write

$$\frac{[\psi(0)u_e/q_e^2\delta^*]_c}{(\sigma/q_e)_i^2\epsilon_T^2}=\frac{2}{\pi}(\bar{k}) \tag{18}$$

We recognize that the right-hand side of the above is constant, as well as $(\sigma/q_e)_i$ which has a value of 0.006. Inasmuch as the compressibility factor ϵ_T is an inverse function of Mach number (Fig. 1), then the zero intercept value for compressible flow should decrease with increasing M_e. Moreover, use of the incompressible formulation for PSD via the Houbolt format that considers q_e^2 instead of σ^2 for normalization should allow for compressible data to be transformed into the incompressible plane using the compressibility factor. Figure 6 shows the results from several compressible experiments as well as the incompressible data of Bull and Blake. The compressible data indicate that the zero intercept values are indeed less than the incompressible value (2.29×10^{-5}). Hence, Eq. (18) will serve as the basis for which compressible data will be evaluated in the current investigation.

Some comments are in order relative to gage size and measuring errors in the high-frequency range. Willmarth[2] noted that earlier investigations (prior to Blake) used large transducers that could not resolve small-scale fluctuations even when using gage size corrections. Figure 5 shows such a disparity between the data of Bull and Blake for Strouhal numbers >1. Bull and Thomas[18] performed an experiment to determine the difference between pinhole microphone measurements (such as Blake) and piezoelectric transducers as used previously. It was found that the pinhole caused spurious contributions to $\psi(\omega)$, up to factors of 4. Consequently, assuming some error in the Bull data such that the integrated area of the spectra would yield slightly higher values of σ/q than the measured values (0.005), we will assume that the normalized power magnitude has a value of 0.006 for incompressible flow. This appears to be a reasonable choice due to the possible high-frequency errors from both experiments. Hence, use of the above value for σ/q_∞ and $\bar{k}=$ unity yields the desired result for the zero intercept value. When these values are used in Eq. (16), the Houbolt format fits the Bull data over his predicted range $0.2<\omega\delta^*/u_e<20$.

It is observed that a significant dispersion of the data occurs for Strouhal numbers $<5\times10^{-2}$. Due to the high velocities attained at hypersonic conditions the compressible Strouhal number can be less than the incompressible values by over an order of magnitude. This is reflected in the compressible data. Moreover, Dods and Hanly[21] noted that at low frequencies spurious contributions are accorded to the pressure fluctuating field from tunnel noise. We have already noted (Fig. 3) that the AEDC von Kármán A and B Facilities are considered high noise level tunnels. Also, Coe et al.[22] recognized that statistical accuracy is reduced in the low-frequency range. Willmarth[2] in his review commented that many experimenters terminate the spectra for $\omega\delta^*/u_\infty<10^{-1}$ because measurements are obscured due to tunnel noise. Other factors leading to spurious results are attributed to exact definitions of the transition zones, vibration modes, surface/gage roughness, pressure gradient, gage size (high-frequency range), and the interaction of turbulence with turbulence.

Generalization of PSD over Frequency Range

Consider again Eqs. (10) and (18) such that

$$\frac{\psi(0)u_e}{q_e^2\delta^*}=\left(\frac{\delta}{q_e}\right)_c^2\frac{2}{\pi}$$

It has been observed that with increasing Mach number, the zero intercept PSD decreases. Consequently, the right-hand side must also decrease with increasing Mach number. Inasmuch as the term (σ/q_e) behaves in this fashion (Fig. 2), continuity of the above expression is maintained. The compressible state can be transformed into the incompressible plane through a transformation function, a practice commonly employed in boundary-layer theory. For example, the skin friction coefficient can be expressed as

$$C_{f_i}=C_{f_c}F_c$$

where F_c is the transformation function. The rms pressure has been transformed by such a process and is represented by Eq. (10) where $F_c=1/\epsilon_T$. The above zero intercept level can then be written as

$$\frac{\psi(0)u_e}{q_e^2\delta^*}=\frac{2}{\pi}\frac{(\sigma/q_e)_i^2}{F_c^2}=\frac{2}{\pi}\left(\frac{\sigma}{q_e}\right)^2\epsilon_T^2$$

For incompressible flow, one has

$$\left(\frac{\psi(0)u_e}{q_e^2\delta^*}\right)_i=\frac{2}{\pi}\left(\frac{\sigma}{q_e}\right)_i^2\bar{k}$$

Hence, comparing the above expressions allows for the arbitrary parameter $\bar{k}$ to be equal to the compressibility parameter ϵ_T^2. The Strouhal number can also be transformed to

$$\left(\frac{\omega l}{V}\right)_i=F_c\left(\frac{\omega l}{V}\right)_c$$

where $F_c=1/\epsilon_T=1/(\bar{k})^{1/2}$. Equation (16) becomes

$$\left(\frac{\psi(\omega)u_e}{q_e^2\delta^*}\right)_c=\frac{(\sigma/q_e)_i^2\epsilon_T^2(2/\pi)}{1+(1/\epsilon_T^4)(\omega\delta^*/u_e)_c^2} \tag{19}$$

where it is noted that the Strouhal number maintains compressible values. The above formulation represents the power spectral density, in which the Houbolt functional relation has been generalized for application to attached compressible turbulent boundary-layer flow. Here, one notes that both the dependent variable (PSD) and independent variable (Strouhal number) have the required transformation functions.

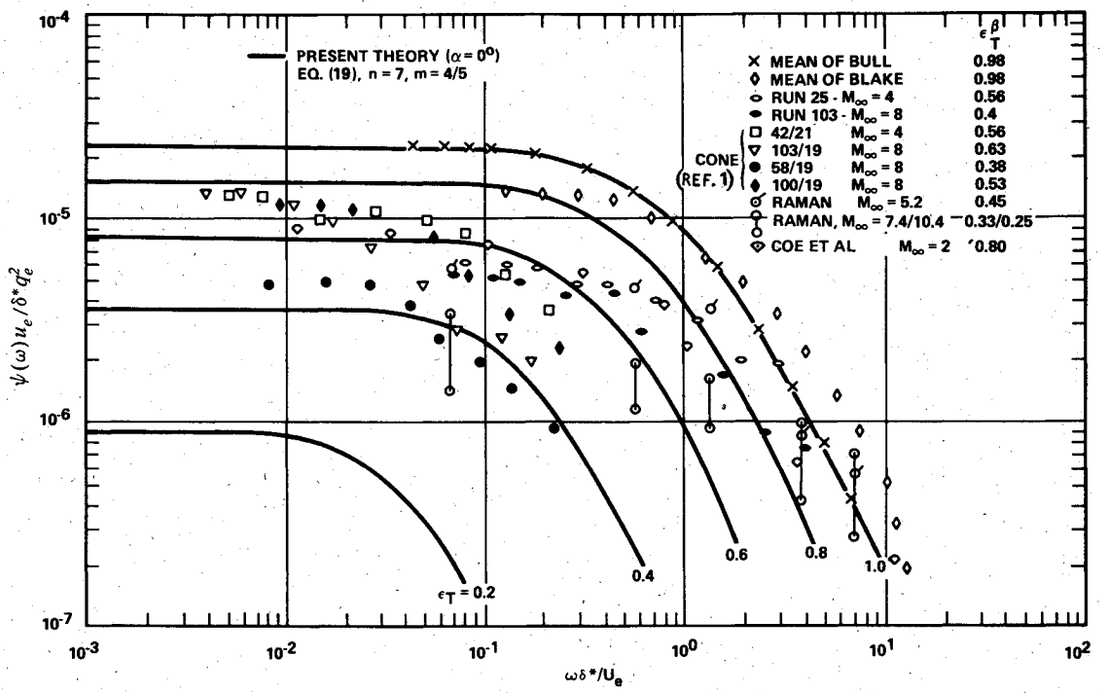

Fig. 7 Comparison of present normalized spectral measurements with other spectral data and theory.

Figure 7 shows the present prediction scheme compared to the data of several experiments and an excellent match to data is observed. The zero intercept value of measured normalized PSD decreases with increasing Mach number and the theory is shown to be in agreement with this trend. However, the decrease of the spectrum with increasing Strouhal number displays different characteristics among the various investigators.

For predicting levels of power spectral density, normalization by edge dynamic pressure and the Houbolt functional form are recommended. The prediction method is shown as Eq. (19) where the compressibility parameter has been employed to transform the incompressible theory into a compressible plane. Of particular importance is the transformation on the independent variable (Strouhal number).

Conclusions

The following algorithms are recommended to describe the pressure fluctuation environment for pressure magnitude and power spectral density for attached turbulent boundary-layer flow.

rms pressure:

$$(\sigma/q_e)_c = (\sigma/q_e)_i \epsilon_T$$

where

$$(\sigma/q_e)_i = 0.006, \text{ incompressible value}$$

$$\epsilon_T = \text{compressibility factor} = (T^*/T_e)^{[2m-(1+n)]/(3+n)}$$

for m and n in the viscous law and velocity power exponents, respectively. The reference temperature ratio T^*/T_e is given by Eq. (4) in terms of local boundary layer properties.

Power spectral density:

$$\left(\frac{\phi(\omega)u_e}{q_e^2\delta^*}\right)_c = \frac{(2/\pi)(\sigma/q_e)_i^2\epsilon_T^2}{1+(1/\epsilon_T^4)(\omega\delta^*/u_e)_c^2}$$

In the above, the fluctuating pressure characteristics described by incompressible flow behavior were modified to a compressible state through a transformation function, a practice commonly employed in boundary-layer theory. The prediction schemes have been compared to both compressible and incompressible wind-tunnel data where good agreement was accorded.

References

[1] Laganelli, A. L. and Howe, J. R., "Prediction of Pressure Fluctuations Associated with Maneuvering Re-Entry Weapons," AFFDL-TR-77-59, July 1977.

[2] Willmarth, W. W., "Pressure Fluctuations Beneath Turbulent Boundary Layers," *Annual Review of Fluid Mechanics*, Vol. 7, 1975.

[3] Raman, K. R., "Surface Pressure Fluctuations in Hypersonic Turbulent Boundary Layers," AIAA Paper 73-997, Oct. 1973 (also NASA CR2386, Feb. 1974).

[4] Laganelli, A. L., Martellucci, A., and Shaw, L., "Prediction of Surface Pressure Fluctuations in Hypersonic Turbulent Boundary Layers," AIAA Paper 76-409, presented at 9th Fluid/Plasmadynamics Conference, San Diego, Calif., July 1976.

[5] Lilley, C. M., "A Review of Pressure Fluctuations in Turbulent Boundary Layers at Subsonic and Supersonic Speeds," *Archiwum Mechaniki Stosowanej*, No. 16, 1964, p. 301.

[6] Kistler, A. L. and Chen, W. S., "The Fluctuating Pressure Field in a Supersonic Turbulent Boundary Layer," *Journal of Fluid Mechanics*, Vol. 16, Pt. 1, 1963, pp. 41-64.

[7] Martellucci, A., Chaump, L., Rogers, D., and Smith, D., "Experimental Determination of the Aeroacoustic Environment about a Slender Cone," *AIAA Journal*, Vol. 11, May 1973, pp. 635-642.

[8] Laganelli, A. L., Fogaroli, R. P., and Martellucci, A., "The Effects of Mass Transfer and Angle of Attack of Hypersonic Turbulent Boundary Layer Characteristics," AFFDL-TR-75-35, April 1975 (also AIAA Paper 77-784, June 1977).

[9] Laganelli, A. L., "Evaluation of Turbulent Heating Predictions," General Electric Rept. TIS 72SD229, June 1972 (also NASA CR130251, Nov. 1972).

[10] Lowson, M. V., "Prediction of Boundary Layer Pressure Fluctuations," AFFDL-TR-67-167, April 1968.

[11] Houbolt, J. C., "On the Estimation of Pressure Fluctuations in Boundary Layers and Wakes," General Electric Rept. TIS 66SD296, April 1966.

[12] Murphy, D. A., Bies, D. A., Speaker, W. W., and Franken, P. A., "Wind Tunnel Investigation of Turbulent Boundary Layer Noise as Related to Design Criteria for High Performance Vehicles," NASA TN D-2247, April 1964.

[13] Stainback, P. C. and Rainey, R. A., "Correlation of Freestream Pressure Disturbances in Supersonic Wind Tunnels," *AIAA Journal*, Vol. 14, Feb. 1976, p. 286.

[14] Donaldson, J. C., Arnold Engineering Development Center, Unpublished results from Tunnel B (Mach 8), private communication, April 1976.

[15] Laderman, A. J., "Review of Wind Tunnel Freestream Pressure Fluctuations," *AIAA Journal*, Vol. 15, April 1977, p. 605.

[16] Bull, M. K., "Wall-Pressure Fluctuations Associated with Subsonic Turbulent Boundary Layer Flow," *Journal of Fluid Mechanics*, Vol. 28, Pt. 4, 1967.

[17] Blake, M. K., "Turbulent Boundary Layer Wall Pressure Fluctuations on Smooth and Rough Walls," *Journal of Fluid Mechanics*, Vol. 44, Pt. 4, Dec. 1970.

[18] Bull, J. K. and Thomas, A.S.W., "High Frequency Wall Pressure Fluctuations in Turbulent Boundary Layers," *The Physics of Fluids*, Vol. 19, April 1976, p. 597.

[19] Robertson, J. E., "Prediction of In-Flight Fluctuating Pressure Environments Including Protuberance Induced Flow," Wyle Laboratories Research Rept. WR-71-10, March 1971.

[20] Schloemer, H. H., "Effects of Pressure Gradients on Turbulent Boundary Layer Wall Pressure Fluctuations," *Journal of Acoustical Society of America*, Vol. 42, 1967, pp. 93-113.

[21] Dods, J. B., Jr., and Hanly, R. D., "Evaluation of Transonic and Supersonic Wind Tunnel Background Noise and Effects of Surface Pressure Fluctuation Measurements," AIAA Paper 72-1004, Sept. 1972.

[22] Coe, C. F., Chyu, W. J., and Dods, J. B., "Pressure Fluctuations Underlying Attached and Separated Supersonic Turbulent Boundary Layers and Shock Waves," AIAA Paper 73-996, Oct. 1973.